

**INTERNATIONAL JOURNAL OF ENGINEERING SCIENCES & MANAGEMENT**  
**SYNTHESIS AND CHARACTERIZATION OF TiO<sub>2</sub> NANOCRYSTALS BY SOL-GEL METHOD AND TO STUDY THE EFFECT OF CALCINATION TIME ON THE ITS PHOTOCATALYTIC ACTIVITY**

**Vipul Shinde<sup>1</sup> and S. B. Bajaj<sup>1,\*</sup>**

<sup>1</sup>J E S Society's R G Bagdia Arts, S B Lakhotia Commerce and R Bezonji Science College,  
Jalna, Maharashtra, India 431203

**ABSTRACT**

TiO<sub>2</sub> nanoparticles were prepared by a simple sol-gel method at different calcinations time. The prepared samples were characterized by X-ray diffraction and UV visible spectroscopy techniques. The formation of hydroxyl radicals ( $\bullet$ OH) on the surface of UV light illuminated TiO<sub>2</sub> nanoparticles was detected by UV visible absorption spectroscopic technique. The photocatalytic activity was evaluated by photocatalytic decolorization of Methylene Blue (MB) aqueous solution under UV light irradiation. The results revealed that the TiO<sub>2</sub> could be crystallized via sol-gel method. The light absorption, the formation rate of hydroxyl radicals, and photocatalytic decolorization of MB aqueous solution were significantly enhanced for mixed phase instead of simple anatase or rutile phase.

**Keywords:** TiO<sub>2</sub>, photocatalytic, degradation, sol-gel, calcination.

**I. INTRODUCTION**

Semiconductors having band gap energies adequate for endorsing and catalyzing a broad range of chemical reactions are of environmental importance [1]. Among many semiconductors, TiO<sub>2</sub> has established to be the most suitable for prevalent environmental applications because of its biological and chemical unresponsiveness, constancy against photo corrosion and chemical corrosion, and cost-efficiency [2-5]. Most important is its photocatalytic property which enables its application for the purification of water, self-consciousness of growth of unwanted microbes and self cleaning surfaces [6,7]. The photocatalytic process involves the degradation of the organic pollutant when TiO<sub>2</sub> is irradiated with Ultra Violet (UV) light in presence of the aqueous solution of the organic pollutant. Fujishima and Honda in 1972 reported the photocatalytic activity of TiO<sub>2</sub> for the first time. Since then, there has been a great research going on in this field. To boost the photocatalytic activity of TiO<sub>2</sub>, several methods have been discovered. The photocatalytic efficiency of TiO<sub>2</sub> particles largely depend upon their microstructure, crystalline structure, particle size as well as on the impurities present. Because of these factors the preparation conditions have large influence on its photocatalytic efficiency. Nanostructures of TiO<sub>2</sub> are investigated on a large scale as they possess high specific surface area which is used up for degradation. The role of different crystalline phases of TiO<sub>2</sub>, mainly

anatase and rutile phase has also been extensively studied in respect of TiO<sub>2</sub>/UV process. Anatase phase is found to be showing highest photocatalytic activity. However, the composition of different phases, are reported to show better photocatalytic degradation. Degussa P25, is commercially obtainable, shows very good photocatalytic degradation consists of two forms of TiO<sub>2</sub> (approximately 1:3 ratio of rutile : anatase). The proposed mechanism based on generation of electron-hole couples with strong redox properties has been used as a platform to explain the differences in the photocatalytic efficiencies observed in these systems [8]. Extensive work has also been carried out in order to improve the photocatalytic efficiency of nanoparticles of TiO<sub>2</sub> by using different techniques like doping and using support catalyst. Support catalyst such as graphite [9,10], carbon nanotubes (Yao) and activated carbon [11,12]. Doping lead to the formation of interstitial sites which act as trapping sites and thus, increase the recombination time. This increases the possibility of redox reactions. Support catalyst has impact on the growth phenomenon and hence it controls various phase formations. It forms junction with TiO<sub>2</sub> and hence controls the flow of charge carriers.

In this paper TiO<sub>2</sub> powder was synthesized by sol-gel method. The sol formed was calcined at different time. Different phase formation and crystallite size was observed. The activity of TiO<sub>2</sub> was studied by observing photocatalytic degradation of methylene blue (MB) under UV light. Calcination time was optimized by observing photocatalytic degradation of methylene blue (MB). Several batches of synthesis were carried on. The work is important as here we got positive results for particular time. Also, the change in crystalline nature is vital, as it can be used to control the phase of TiO<sub>2</sub>. This paper includes the theoretical background of the work, the

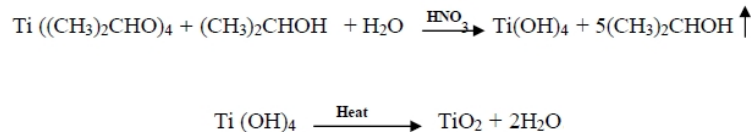
experimental techniques involved in the work and the detailed results of the experiment. The conclusions are discussed in detail on the basis of theory and observed results.

## II. EXPERIMENTAL

TiO<sub>2</sub> was synthesized using Sol-Gel method using titanium alkoxide as a starting material. Titanium alkoxide in isopropyl alcohol form sol through the process of the hydrolysis i.e. the small particle of hydroxide of titanium get dispersed in the solution to form sol. This sol when further reacted undergoes gelation giving nanocrystalline porous gel. Then nanocrystalline porous gel is heated to convert it into crystallites. Titanium dioxide (TiO<sub>2</sub>) powder was prepared by a Sol-Gel (SGS) technique.

Chemicals: Titanium tetra isopropoxide [(Ti(OCH(CH<sub>3</sub>)<sub>2</sub>)<sub>4</sub>)] (Spectrometer Pvt. Ltd. Mumbai, Mol. Wt. 284.25), Isopropyl alcohol [(CH<sub>3</sub>)<sub>2</sub>CHOH] (Thomas Baker, Mol. Wt. 60.10), Nitric acid [HNO<sub>3</sub>] (Thomas Baker, Mol. Wt. 63.01) and Double Distilled water [H<sub>2</sub>O].

We have taken the weight ratio of [(Ti(OCH(CH<sub>3</sub>)<sub>2</sub>)<sub>4</sub>)] : (CH<sub>3</sub>)<sub>2</sub>CHOH : H<sub>2</sub>O : HNO<sub>3</sub> as 1:10:1:0.2 for the formation of SGS in order to synthesize TiO<sub>2</sub>. 40ml isopropyl alcohol (IPA) was taken in a beaker and titanium tetra isopropoxide (TTIP) was added dropwise in it which act as a precursor of TiO<sub>2</sub> in this reaction. During the addition of TTIP to IPA continuous stirring is required. After 30 minutes of stirring at room temperature, solution is kept at constant temperature of 80°C. 0.8 ml of 10% HNO<sub>3</sub> and 4 ml distilled water is then added drop wise with continuous stirring. After addition of water, solution forms gel structure. This gel like structure is due to formation of Ti(OH)<sub>4</sub> linkage as shown in the reaction below. This gel was stirred at 80°C till it sufficiently dried to become paste. This paste was kept in furnace (Indfurthyristorised furnace, 4.5 kW) for calcination to get nanocrystalline TiO<sub>2</sub>. We have synthesized TiO<sub>2</sub> for different calcination temperatures (250°C to 750°C instead of 1000°C) at constant calcination period. Six samples were prepared which were subjected to photocatalytic degradation. The calcination temperature at which maximum degradation was kept constant for further synthesis. The samples obtained were, then used to observe photocatalytic degradation. The calcination temperature was optimized, based on photocatalytic activity.



## III. RESULTS

### X-ray Diffraction:

As synthesized samples of TiO<sub>2</sub>, were characterized by XRD, to study the detailed crystalline nature of particles and their phase formation. The XRD measurements were performed on a X-ray diffractometer using Cu K $\alpha$  irradiation ( $\lambda=0.154\text{nm}$ ). Data were recorded for a range of 20° to 80° with a step width of 0.1°. We have investigated the structural transformations of a mixed anatase-rutile nanocrystalline TiO<sub>2</sub> nano particles in effect of the annealing temperature. The determination of TiO<sub>2</sub> phase and the crystallite size upon isochronal and isothermal calcination the powder in air at temperatures ranging from 250°C to 750°C in steps of 100°C was done by XRD technique. We can calculate percentage of phases in the sample. In order to quantify that XRD peak intensity ratios were used. The ratio between anatase and rutile extracted from XRD spectra was computed with the empirical relationship [10].

$$R(T) = 0.679 \left( \frac{I_R}{I_R + I_A} \right) + 0.312 \left( \frac{I_R}{I_R + I_A} \right)^2$$

where,

$R(T)$  is the percentage content of rutile at each temperature,

$I_A$  is the intensity of the main anatase reflection (101) ( $2\theta=25.30^\circ$ ), and

$I_R$  is the intensity of the main rutile reflection (110) ( $2\theta=27.44^\circ$ ).

The X-ray diffraction pattern of TiO<sub>2</sub> calcined at different temperatures is shown in Figure 1. The lower two curves show the X-ray diffraction peaks of anatase and rutile phases of TiO<sub>2</sub> as reported in the X-ray diffraction data files (JCPDS). Remaining graphs are the X-ray diffraction graphs of as synthesized samples with decreasing calcination temperatures as we see from lower graph to upper graph as indicated in the Figure 1. From Figure 1, it is observed that for lower calcination temperatures the X-Ray diffraction peaks have larger fullwidth half maximum indicating

lesser crystalline nature. As calcination temperature increases, peaks become narrow, as a result of increased crystalline nature. This is also evident from the crystallite size calculations by Sherrer formula shown in Table 1. With increase in calcination temperature, the crystallite size increases. It can also be seen that at lower temperature, percentage of anatase phase, which is a metastable state, is higher while percentage of rutile phase is lower. As temperature increases, percentage of anatase decreases and percentage of rutile increases.

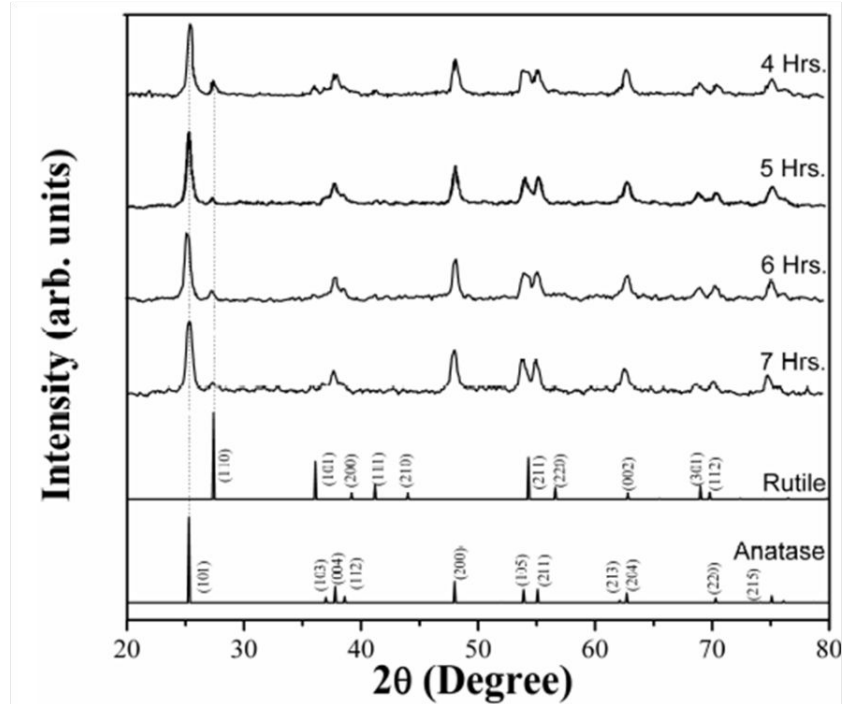


Figure 1: X-ray diffraction pattern of as synthesized samples of  $\text{TiO}_2$  at different calcination time.

#### UV-Visible absorption:

UV-Visible absorption spectroscopy was used for determining the band structure of the as synthesized samples. Also, it was used to observe the photocatalytic degradation. Figure 2 shows the UV-Visible absorption spectra of as synthesized  $\text{TiO}_2$  samples calcined at different temperatures. It can be observed from the graph that as the calcinations temperature is increased the defect states decrease. This is also in accordance to XRD analysis. With increase in calcination temperature the crystallinity increases, thus the amorphous nature decreases and hence the defect states decrease. The sharp fall in absorbance is maximum for the sample calcined at  $750^\circ\text{C}$  and the band gap is found to be 2.96 eV. The band gap values as observed from the graph are written in Table 1.

#### Degradation:

Figure 3 shows the UV-Visible absorption graph of MB. The absorption of MB is maximum at wavelength 664 nm. As the concentration of MB is decreased the absorption also decreases. Hence, relative change in concentration of MB can be observed by absorption measurements. Here, the pink curve corresponds to the absorption curve of 10-5M solution of MB. The other curves correspond to the absorption curves of MB same solution treated with  $\text{TiO}_2$  particle under UV light exposure for 30 min. It was observed that the maximum degradation (means minimum absorption) was shown by  $\text{TiO}_2$  calcined at  $550^\circ\text{C}$ .

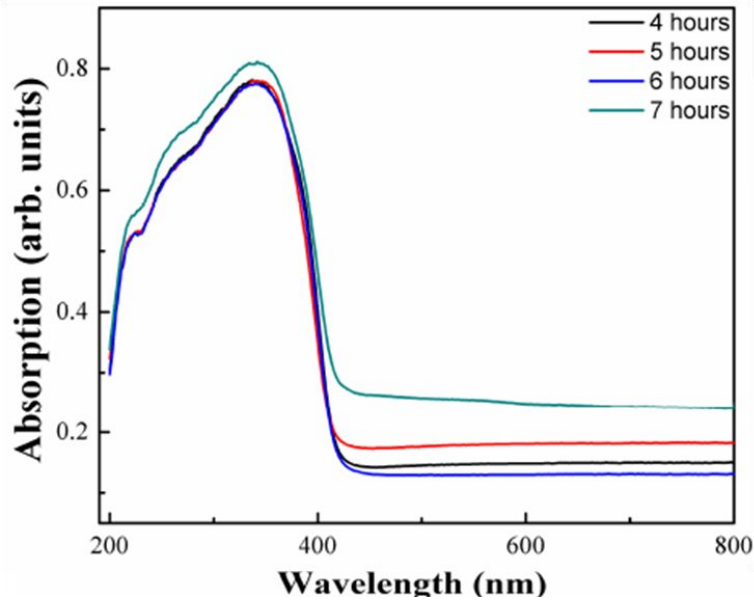


Figure 2: UV-Visible absorption spectra of synthesized  $TiO_2$  samples calcined at different time.

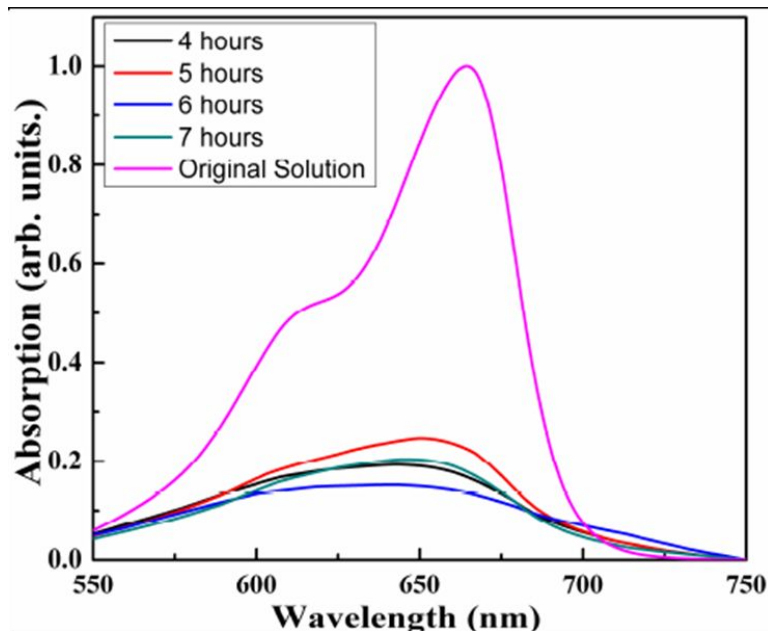


Figure 3: UV-Visible Absorption graph of MB after degradation using as synthesized  $TiO_2$  samples calcined at different time.

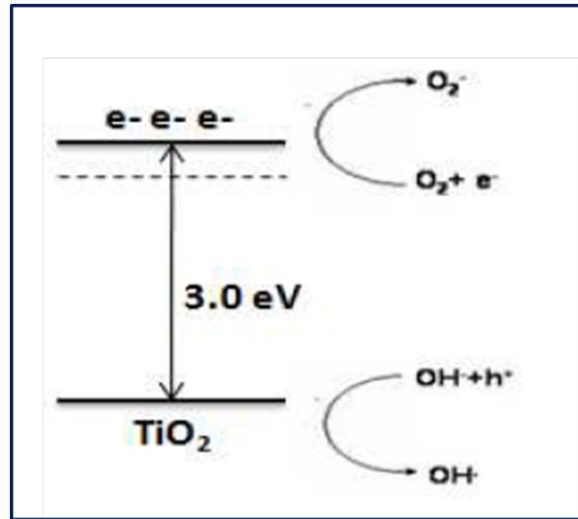


Figure 4: Redox reactions that take place at the surface of (bulk)  $\text{TiO}_2$ .

#### IV. DISCUSSIONS

Photocatalysis over a semiconductor oxide such as  $\text{TiO}_2$  is initiated by the absorption of a photon with energy equal to or greater than the band gap of the semiconductor, producing electron-hole ( $e^-/h^+$ ) pairs. Consequently, following irradiation, the  $\text{TiO}_2$  particles can act as either an electron donor or acceptor for molecules in the surrounding medium. The electron and hole can recombine, releasing the absorbed light energy as heat, with no chemical effect. Otherwise, the charges can move to "trap" sites at slightly lower energies. The charges can still recombine, or they participate in redox reactions with adsorbed species. A simplified mechanism for the photo-activation of a semiconductor catalyst is presented in figure 4. The valence band hole is strongly oxidizing, and the conduction band electron is strongly reducing. At the external surface, the excited electron and the hole can take part in redox reactions with adsorbed species such as water, hydroxide ion ( $\text{OH}^-$ ), organic compounds, or oxygen. The charges can react directly with adsorbed pollutants, but reactions with water are far more likely since the water molecules are far more populous than contaminant molecules.

There are two routes through which OH radicals can be formed. The reaction of the valence-band "holes" ( $h^+_{\text{vb}}$ ) with either adsorbed  $\text{H}_2\text{O}$  or with the surface  $\text{OH}^-$  groups on the  $\text{TiO}_2$  particle.  $\text{H}_2\text{O}$  will adsorb and react with a hole in the valence-band and an acceptor (A) such as dioxygen will also be adsorbed and react with the electron in the

conduction band ( $e^-_{\text{cb}}$ ). Oxygen can trap conduction-band electrons to form superoxide ion ( $\text{O}_2^{\cdot -}$ ). These superoxide

ions can react with hydrogen ions (formed by water splitting), forming  $\text{HO}_2^{\cdot}$ . A competition reaction occurs between water, oxygen, organic molecules and trace metals which may be present in the system. Oxygen molecules will be

reduced and give active species ( $\text{O}_2^{\cdot -}$ ). Water will be oxidized by the hole in the valence band to give the very

active free radical  $\cdot\text{OH}$  which can oxidize organic species.

Table:

Table 1. Details of as synthesized samples of  $\text{TiO}_2$  at different calcinations time.

Sr. No.	Calcination Time (Hrs)	Anatase (%)	Rutile (%)	A/R ratio	Crystallite size (nm)	BandGap (eV)
Error	-		±1%		±0.5 nm	±0.1 eV
1	4	90	10	9.00	35.39	3.03
2	5	88	12	7.33	32.56	3.04
3	6	87	13	6.69	29.07	3.05
4	7	85	15	5.67	27.13	3.08

## V. CONCLUSION

TiO<sub>2</sub> nanoparticles can be facilely prepared by a simple sol-gel method at different calcination time and assisted with photodegradation technique. Results show as the calcination time to some extent increases crystallinity, size and band gap remains almost comparable. Moreover, degradation is higher for 6 hours calcination time. The finding of this work is, the absorption of light, the hydroxyl radicals formation rates, and photocatalytic degradation of MB aqueous solution were significantly dependant on particular percentage of anatase to rutile ratio. Only anatase or rutile phase shows less degradation rate as compare to mixed phase.

## REFERENCES

- [1] M. R. Hoffman, S. T. Martin, W. Choi and D. W. Bahnemann, *Chem. Rev.* (1995) 95, 69.
- [2] J. Moon, H. Tagaki, Y. Fujishiro and M Awano, *J. Mater. Sci.* (2001) 36, 949.
- [3] I.P. Parkin and R.G. Palgrave, *J. Mat. Chem.* (2005) 15, 1689.
- [4] B. Levy, *J. Electrocer.* (1997) 1, 239.
- [5] A.G. Agrios and K.A. Gray, *Environmental Catalysis* (2005) 369.
- [6] N. Negishi, T. Iyoda, K. Hashimoto and A. Fujishima, *Chem. Lett.* (1995) 841.
- [7] Y. Anjaneyulu, N. S. Chary and D. Samuel, S. Raj, *Rev. Environ. Sci. and Bio tech.* (2005) 4, 245.
- [8] A. Fujishima, T. N. Rao and D. A. Tryk, *J. Photochemistry and Photobiology C: Photochemistry Reviews* (2000) 1, 1.
- [9] L. W. Zhan, H. B. Fu and Y. F. Zhu, *Adv. Funct. Mater.* (2008) 18, 2180.
- [10] Z. B. Lei, Y. Xiao, L. Q. Dang, W. S. You, G. S. Hu and J. Zhang, *Chem. Mater.* (2007) 19, 477.
- [11] J. Matos, J. Laine and J. M. Herrmann, *Appl. Catal. B* (1998) 18, 281.
- [12] W. D. Wang, C. G. Silva and J. L. Faria, *Appl. Catal. B.* 70 (2007) 470.
- [13] Kazuhito Hashimoto, Hiroshi Irie and Akira Fujishima *AAPPS Bulletin* (2007) 17, 6.
- [14] J.M. Herrmann, C. Guillard, P. Pichat (1993) 17, 7.
- [15] Karran Woan, Georgios Pyrgiotakis and Wolfgang Sigmund et al *Adv. Mater.* (2009) 21, 2233.
- [16] Jin Chul Kim, Jungkweon Choi, Yong Bok Lee, Jung Hoon Hong, Jong In Lee, Jin Wook Yang, Wan In Lee and Nam Hwi Hur *Chem. Commun.*, 2006, 5024.
- [17] Y. Anjaneyulu, N. Sreedhara Chary and D. Samuel Suman Raj *Reviews in Environmental Science and BioTechnology* (2005) 4, 245.
- [18] Hubert Gnaser, Adam Orendorz, and Christiane Ziegler *Phys. Status Solidi A* (2011) 208, 1635.
- [19] Kazuhito Hashimoto, Hiroshi Irie and Akira Fujishima *J. App. Phy.* (2005) 44, 8269.
- [20] Wonyong Choi, *Catalysis Surveys from Asia et al* (2006) 10, 1.
- [21] Pusit Pookmanee and Sukon Phanichphant et al *Journal of Ceramic Processing Research.* (2009) 10, 167.
- [22] L. E. Depero, L. Sangaletti, B. Allieri, E. Bontempi, R. Salari, M. Zocchi, C. Casale, and M. Notaro, *J. Mater.* (1998) 13, 1644.